19 Magnetic Satiety System: The Use of Magnets to Assist in Combating Obesity

Shahriar Sedghi, Katherine Kendrick, Sheng-Chiang Lee, Samuel Engle, Kenji Yoshida, and Betsy Smith

Obesity Epidemic

Obesity is routinely defined as an excess of body weight for height [1]. This is quantified as a body mass index (BMI), which is calculated by body weight in kilograms divided by height in meters squared. In adults, a BMI of greater than or equal to 25 is considered overweight, and a BMI of 30 is considered obese. Current estimates predict that that the rapid rise in obesity will continue to soar and that 3/4 of the American population will likely be overweight or obese by 2020 [2, 3]. A report by the Trust for America's Health and the Robert Wood Johnson Foundation found, using a model of population and trends, that half of US adults will be obese by 2030 [1]. In 2014, the National Health and Nutrition Examination Survey found that more than one-third (36.5%) of US adults aged 20 and older and 17% of children and adolescents aged 2–19 were obese. These figures are on the rise. The rapid rise in obesity over the twentieth century is concerning because obesity is associated with a decrease of lifespan by 4–7 years, increased risk of nearly every chronic disease, as well as increased morbidity and mortality [1].

Obesity has been found to contribute to more than 3 million deaths per year [4]. It is now the leading cause of morbidity and mortality in Western societies [5]. It has been found that, in men aged 25–34 years with a BMI >40 kg/m^2, there is a 10-fold excess mortality compared with their normal weight counterparts [6]. The current US generation is predicted to have a shorter life expectancy than their parents, due to the association of obesity and risk of nearly every chronic disease known [3]. Diseases associated with obesity include metabolic syndrome, diabetes mellitus, hypertension, coronary artery disease, sleep apnea, stroke, gastroesophageal reflux disease, certain malignancies, and fatty liver disease [5–7]. Obesity is additionally associated with increased aging [6]. The increase in obesity and obesity-related disease is taking a toll on healthcare costs. Obesity currently accounts for 17% of healthcare costs in the United States. Healthcare costs are significantly increased for both obese males and females [8]. The total US healthcare

S. Sedghi (✉)
Appetec INC, Gastroenterology Associates of Central Georgia, Macon, GA, USA

K. Kendrick
Department of Internal Medicine, Navicent Health/Mercer University School of Medicine, Macon, GA, USA

S.-C. Lee
Appetec INC, Macon, GA, USA

S. Engle
Business Development, Synectic Medical Product Development, Woodbridge, CT, USA

K. Yoshida
Clinical/Research, Gastroenterology Associates of Central Georgia, Macon, GA, USA

B. Smith
Department of Internal Medicine, Mercer University School of Medicine, Macon, GA, USA

M. Gagner (ed.), *Magnetic Surgery*, https://doi.org/10.1007/978-3-030-73947-8_19

spending is estimated at $2.7 trillion [1]. An additional cost is related to loss of productivity in the workplace. When examined in 2012, a company's annual healthcare cost and lost productivity in the highest vs lowest BMI groups was reported to be $6,313 with an average of 7.5 missed days versus $4,258 with an average of 4.5 days, respectively [8].

The question seldom asked is, why is there an obesity epidemic? After the 1980s, there was a significant rise in obesity [8, 9]. The increase has been attributed to "built environment," which includes the development of products that reduce physical activity that is, elevators, escalators, online entertainment, and television [8]. The built environment also includes the industrialization of food production, allowing access to inexpensive, highly processed, nutrient-poor food, as a major contribution. The consumption of sugar was rare prior to 1900, around 4–6 pound per year; currently, the average person consumes ~160 pounds per year [8]. It has been shown that added sugar is not only highly addictive but is also associated with obesity [8, 10]. Billions of dollars each year are allocated to advertising calorie-rich and nutrient-poor foods to children [8].

We now have such high numbers of obese and overweight people that the perception of "normal" is being altered. Social networks are contributing to the standardization of this new norm of being obese or overweight in our population [11]. Restaurants tend to be valued for large portion sizes, and large sugar-filled drinks are considered normal. Eating high-calorie food has been shown to lead to overeating, independent of macronutrient content or portion size [4, 12]. Also concerning is that the Western diet is metabolically toxic, as studies have shown that high-fat foods cause damage to regions of the brain that regulate food intake and can cause insulin resistance [4, 13–15]. Efforts to address the obesity epidemic as a public health issue in the United States have been labeled by many as paternalistic, undemocratic, excessive, and inappropriate. The societal expenses of obesity are considered as acceptable as the cost of personal freedom and choice [8]. It is imperative that any current or future treatment for obesity takes historical and etiological factors into consideration for their innovation to be successful.

Underlying Mechanisms of Obesity

The underlying cause of obesity is disruption of the homeostatic balance between energy intake and energy expenditure. When homeostatic mechanisms controlling food intake are poorly adapted to the unique modern environment of "plenty," both excess energy and reduced exercise result in obesity [16]. The intake of calories is controlled by complex interactions between the gut and central nervous system that are mediated by neural and hormonal signals [7, 16–20]. The brain interprets peripheral signals from the gut and adipose tissue regarding the need for energy intake and responds to such signals by increasing or decreasing food intake as needed. Intricate neuronal networks are housed within key brain areas such as the hypothalamus and brainstem; gut hormones (i.e., ghrelin, leptin, PYY, and GLP-1) act upon these neural networks which subsequently connect to other areas of the brain involved in feelings of reward and desire. Involvement of such centers within the brain is crucial to the body's response to hunger, satiation, and adjustment of energy intake [21, 22] (Fig. 19.1). Although such mechanisms are used to maintain the delicate balance between energy intake and expenditure, the reward system located in the ventral tegmental area (VTA) of the brain can override this homeostatic mechanism when presented with desirable food that is not necessary for energy balance, and the pleasure that is perceived by eating high-calorie foods reinforces the behavior [4]. Studies have shown the VTA is rich with dopaminergic neurons that are stimulated by food intake [4, 23, 24]. These are the same areas activated by psychoactive drugs, which tells us that food addiction is real[4]. The reward area of the brain also receives inputs from the brainstem and hypothalamus and is adjusted by vagal nerve stimulation [4, 23–25]. The drive for food intake is fundamental to survival [16]. However, the existence of this drive in the context of a surplus of energy within the modern environment has led to the obesity epidemic.

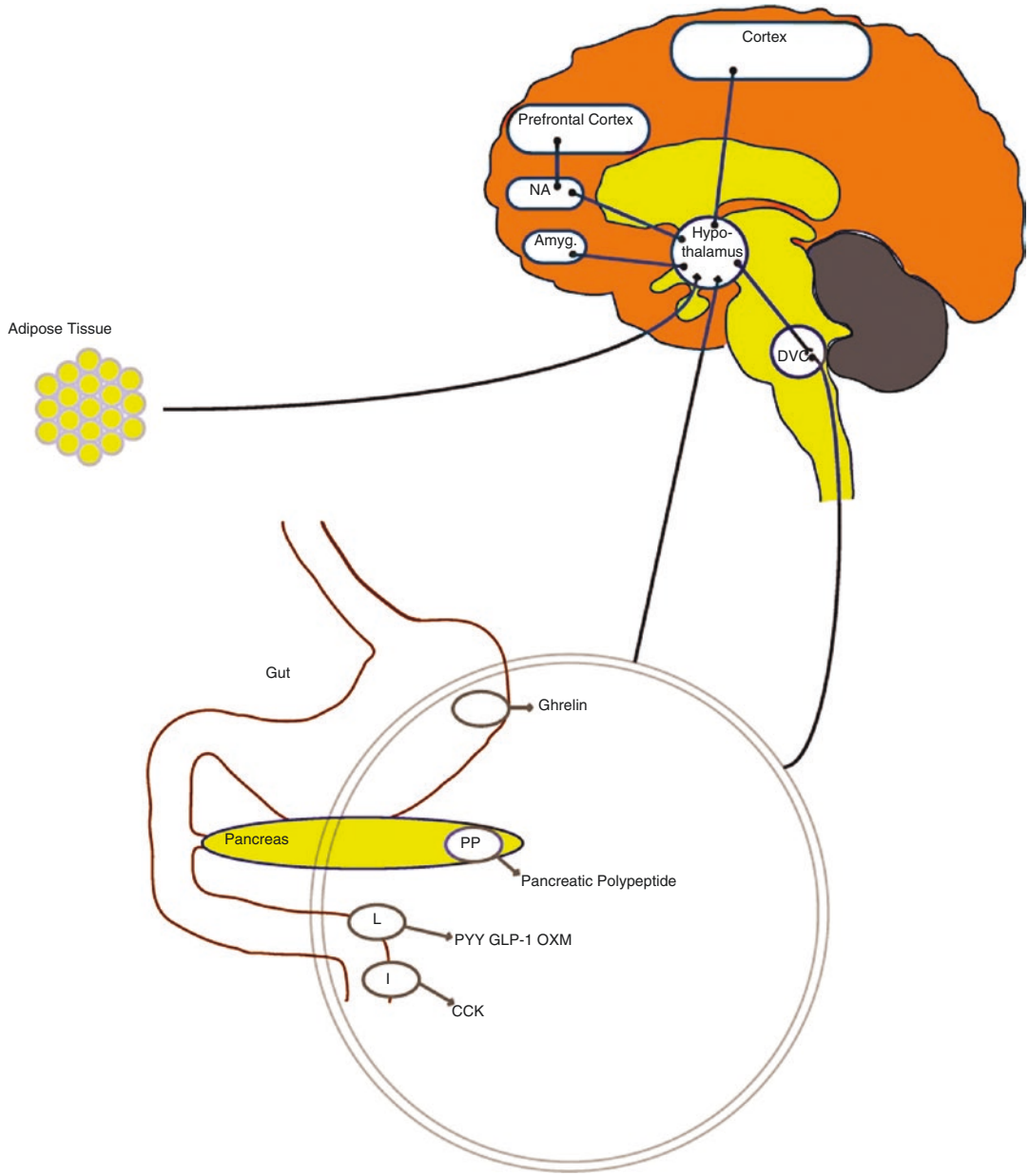

Fig. 19.1 Peripheral signals influence the hypothalamus. Neural projections between the hypothalamus, brainstem, cortex, and reward centers influence food intake. (From Simpson K, Bloom S [16]. Reprinted with permission from Elsevier)

Gastric/Brain Axis and Food Intake

The muscular layers of the stomach house intramuscular arrays in the outer muscular layer and act as stretch receptors and likely mediators of satiation due to their connection with vagal afferents [20, 26]. There are myriad neuroendocrine and exocrine factors involved in the start and cessation of a meal [27–29]. One mechanism that is believed to influence meal termination is via distension of the stomach and subsequent activation of gastric mechanorecep-

tors [27]. Mechanoreceptors, once stimulated, transport their signal along the vagus nerve, and influence the initiation and termination of a meal by conveying to the current digestive state to the nucleus of the solitary tract located in the medulla of the brain stem [4, 27]. Studies have shown distension of the stomach does not affect hunger satiety. However, the limitation of these studies is distension occurred 10 minutes after meals, with the average meal only lasting 12 minutes while an individual is alone [30–34]. Distension of the stomach which contains food will lead to lead to meal termination. The signals are then relayed to other feeding-related areas of the brain, including the hypothalamus [4, 35, 36] and either activate or inhibit orexigenic signals based on the cumulative effect of the brain and gastric inputs [27]. This leads to a feeling of either hunger or fullness in the body, and an alteration in the consumption of food [18, 19, 27, 36–38]. Neuroimaging that examines gastric distention provides potentially valuable information regarding the vagal afferent pathways to visceral cortical areas. Studies in these areas have focused on activation of neural areas associated with painful versus not painful gastric distension [38, 39]. Along with activation of cerebral networks important for food processing, stomach distension also interacts with gut-secreted peptides [22, 40].

During chronic distension of the stomach wall, levels of ghrelin, a hunger-inducing hormone, initially drop, and contribute to satiety [7]. In experiments with healthy subjects receiving either an intragastric load or a continuous intraduodenal infusion of glucose or a mixed liquid meal, the stomach appears to be important in the short-term control of appetite [41]. Results suggest that gastric and intestinal signals interact to mediate early fullness and satiation, likely via interactions of the secretion of ghrelin, leptin, glucagon-like peptide-1 (GLP-1), and peptide YY (PYY) [41]. Animal studies also support these concepts [37–39] and suggest that a combination of gastric signals and intestinal nutrient stimulation is necessary to elicit optimal satiation and adequate control of eating [41].

Studies dating back 50 years have demonstrated that the behavioral response to gastric distension nearly always includes a reduction in food intake [27, 42], whether this distension is due to ingestion of food [27, 43], or acute intragastric balloon inflation. Normal weight humans exhibited a marked decrease in food intake after acute balloon inflation [34], and studies of obese humans who received chronic balloons as a weight-loss therapy showed weight reduction during the first three months [27]. Modulation of neural and hormonal feedback signaling has been suggested as the basis of intragastric balloons for weight loss, although varying results have been found for ghrelin and for other peptides that are modulated [7, 44, 45]. One possible factor contributing to these variations could be the measurement of total ghrelin and the inactive form of this peptide, as well as changes in body weights and reduced food intake which affect ghrelin levels [7, 42]. When balloons are placed chronically, there is at least a short-term weight loss for three to six months, but there is a lack of long-term efficacy [7, 46, 47]. This may be due to physiological or behavioral adaptations along with divergence between gastric pressure and volume with balloon distension [27, 30].

Weight Loss Strategies and Risks

Recidivism is recognized after all approaches to weight loss. Failure is seen with dietary, behavioral, pharmacological, and surgical interventions for weight loss. A variation of diets, which includes Mediterranean, low fat, and calorie restriction (including both low calorie and very low calorie), resulted in a weight reduction of 5–7.8%, but had a rebound weight gain of 41–61% [48]. The weight regain is due to metabolic adaptation and loss of adherence. Pharmacological approaches for weight loss use medications such as phentermine and extended release topiramate, lorcaserin, combination of bupropion and naltrexone, liraglutide, and orlistat. These medications result in only 5–10% loss of body weight in the most successful patients, and the weight tends to be

regained once the medication is stopped [49]. A hindrance to adherence to these medications are the side effects which include, but are not limited to, dry mouth, paresthesia, constipation, dysgeusia, insomnia, and disturbances in cognition, attention, concentration, and memory [48, 49]. Numerous other side effects are associated with each individual drug.

Bariatric surgery was first described in 1969 and is considered the gold standard for morbid obesity [50]. Ileal transposition in 1982 removed a section of the terminal ileum and incorporated it into the duodenum, which was designed to allow ingested nutrients to have earlier contact with ileal cells, to induce the release of GLP-1 and peptide YY, two hormones involved in satiety. Due to associated complications, this is no longer performed. Current methods of bariatric surgery include the laparoscopic banding, which has a mean weight reduction of 15–20%, Roux-en-Y gastric bypass (mean reduction of 25%), and vertical sleeve gastrectomy (mean reduction is 30%) [26]. Complications of these surgeries can include reflux, anastomotic leaks, internal bowel herniation, obstruction, and perforation, nutritional deficiencies, and dumping syndrome. Removal of lap bands is common due to intolerance of nausea and vomiting. Although bariatric surgery is considered the "standard of care" for treatment of severe obesity, long-term efficacy data have shown that more than 20% of patients regain weight and have a recrudescence of obesity-related comorbidities [49]. Protein and nutritional deficiencies and their long-term sequelae in "successful" gastric bypass patients are often understated. The nutritional deficiencies may represent kwashiorkor (Fig. 19.2). Protein malnutrition remains the most severe nutritional complication associated with bariatric surgery [51]. Protein malnutrition is associated with malabsorptive procedures, causing a hospitalization rate of 1% per year, and leads to significant morbidity and poor outcomes [51]. Due to these factors, as few as 1% of patients eligible for these procedures choose to undergo one of them.

Intragastric balloons (IGB) were then developed as a less invasive way for weight loss. Intragastric balloons have been explored as a treatment for obesity since 1985 and were thought to provide an alternative for patients who declined or were not fit for bariatric surgery. A Cochrane review concluded that there are little data to support intragastric balloons' efficacy for weight loss when compared to conventional medical management [48, 52]. These balloons are filled with liquid or gas and cause a space occupation in the stomach to reduce gastric volume and improve satiety. IGB are endoscopically placed in the stomach under sedation. Numerous balloons have been developed since the first IGB was created. Initial reports found some clinical efficacy, but this was short lived, as the effectiveness for weight loss decreased over time as a result of gastric adaptation [53, 54]. Most IGB have reported side effects such as nausea, vomiting, and gastric mucosal damage, thus IGB have not been widely accepted and are a second-line option for patients who are unable to have bariatric surgery [53]. Other methods include Gelesis pill, vagal nerve stimulation and endoscopic methods, such as endoscopic sleeve gastroplasty, Aspire Assist, TransPyloric Shuttle by BaroNova, and the Full Sense Bariatric Device.

Gelesis is a Boston biotech company that created a hydrogel capsule from blend of cellulose and citric acid. The capsule breaks apart in the stomach exposing the matrix, which can absorb 100 times its weight to create space occupation in the stomach. A double-blind placebo-controlled study found that Gelesis weight loss aid participants lost 6.4% of their baseline weight versus 4.4% in the placebo group. Side effects include GI upset such as diarrhea, bloating, abdominal pain, and gas. The price point has not been established [55].

Vagal nerve stimulation was examined in a clinical trial of 233 patients. After 12 months, the experimental group lost an average of 8.5% more excess weight than the control group [56]. However, the experimental group did not meet the primary outcome of a significantly greater percentage of excess weight loss, defined as >10%, compared to the control group. Even though this standard was not met, the FDA Advisory Committee found that 18-month data from the study were supportive of sustained

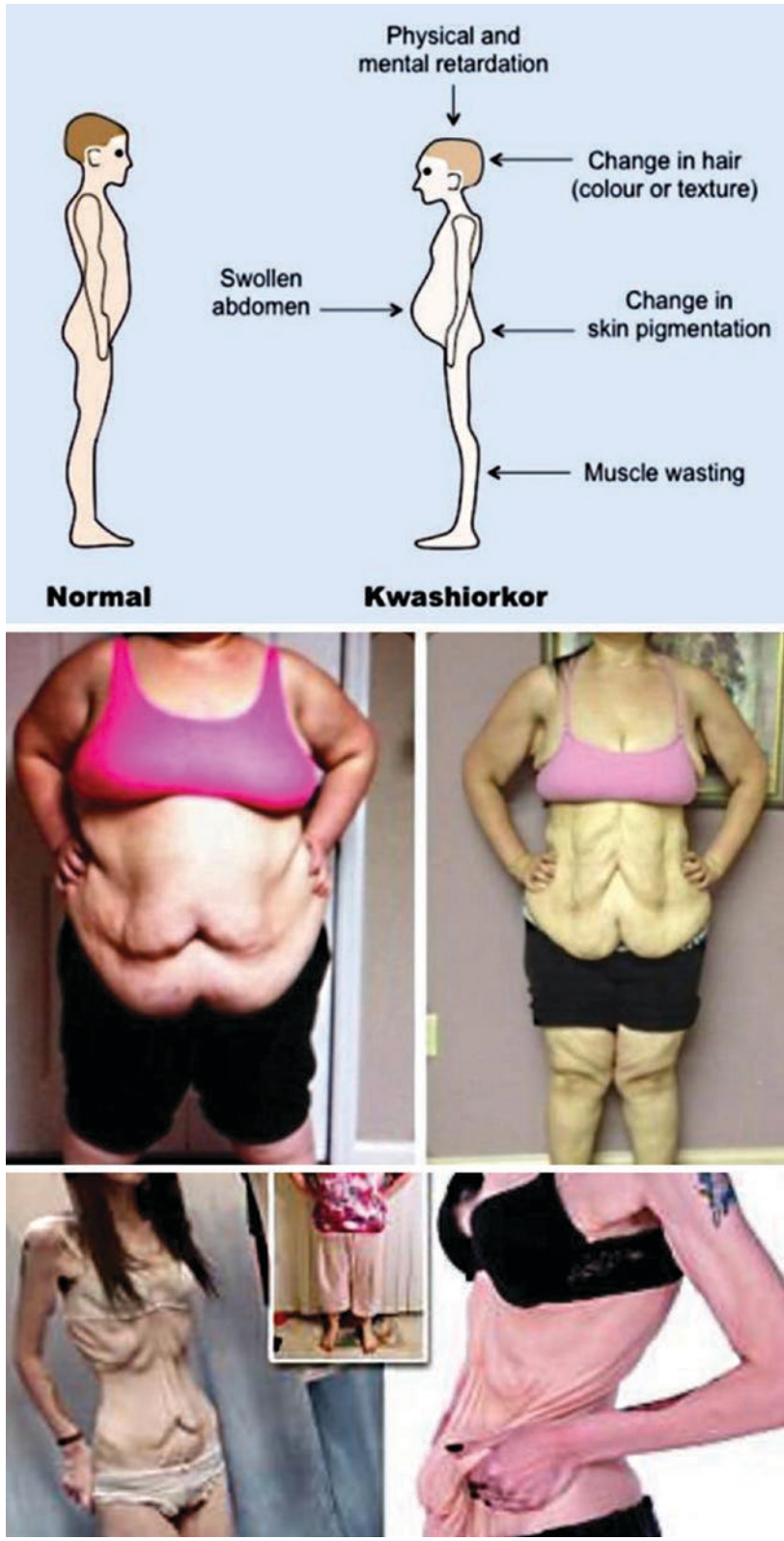

Fig. 19.2 Kwashiorkor description (top panel) and bariatric surgery patient (bottom panels)

weight loss and agreed that the benefits of the device outweighed the risks in patients who met the indication criteria [56]. The approval was based on an FDA-sponsored survey indicating that patients would accept risks associated with the device [56].

Endoscopic methods for weight loss include endoscopic sleeve gastroplasty, which utilized a full-thickness suture to reduce the size of the stomach [57]. Complications from the procedure include nausea, pain, leaks, perforation, perigastric inflammatory fluid collection, splenic laceration, and bleeding [58]. The AspireAssist is a device that placed a tube into the patient's stomach to allow for drainage of the stomach contents after a meal. Drainage of stomach contents is only possible if the patient chews thoroughly and eats slowly [59]. Long-term results of this device are still unknown, and complications include nausea, leaks, perforation, peritonitis, stoma infection, gastric ulceration, and bleeding [59]. BaroNova's TransPyloric Shuttle is placed endoscopically and is designed to slow the passage of food to make the patient feel full sooner and stay full longer. EndoBarrier is a 65-cm long Teflon-coated duodenal jejunal bypass sleeve, which relies on malabsorption for weight loss by allowing undigested food to reach the jejunum. The device was removed from 10.9% of patients in one study due to adverse events [59]. Full Sense Bariatric Device is an esophageal stent connected to a gastric disk via a strut. It is designed to stay in the gastric cardia, in theory, to produce feelings of satiety. Additional procedures being studied include duodenal mucosal resurfacing, to rest the diseased duodenal enteroendocrine cells and self-assembling magnets, which are attempting to divert bile and nutrients to the terminal ileum.

While the aforementioned approaches have demonstrated short-term results, in the absence of unintended surgically induced malabsorption (which is undesirable) or behavioral modification, they lack long-term efficacy. This is because existing techniques do not facilitate noninvasive postoperative adjustment, due to the body's natural adaptation to the surgical and endoscopic changes made. Furthermore, the cornerstone of successful treatment (i.e., behavioral therapy and positive reinforcement) is not incorporated. A study by Spring et al. supports the need for reinforcement and illustrated how mobile technology was of benefit, by demonstrating that remote coaching with mobile technology has a positive impact in overall adoption and maintenance of multiple healthy behavior changes [60]. As a result, both current surgical and endoscopic groups suffer from nonsustained weight loss due to the body's natural adaptation to the changes made, as well as additional complications.

Why There Is a Need for a New Approach

Considering historical evolution of obesity and the recent change in the food industry, which promotes high-caloric and highly addictive food causing failure of the appetite control centers essentially resulting in food addiction, it is easy to see why the current treatments for obesity have been unsuccessful and/or aggressive. An ideal device for obesity management would utilize the existing neurohormonal pathways described above and reinforce the natural physiology of eating, which is intermittent distension, as opposed to some of the currently available products which use chronic distension, restrictive, or obstructive procedures. It has also been theorized that unless the patient is actively involved with treatment of their obesity, long-term efficacy results would be minimal.

These requirements lead to the innovation of Endoscopic Magnetic Appetite Control System (EMACS) by Appetec INC. utilizing magnets. EMACS is an endoscopically placed, free-floating expandable silicone stent with an internal magnet that is manipulated by an external magnet (Fig. 19.3). The external magnet is manipulated by the patient on demand and supervised with an integrated platform. EMACS is minimally invasive, has the potential for use in young adults where food addiction potentiates, and empowers the patient to curb their appetite. Additionally, the device provides positive reinforcement and integrated behavioral therapy that is not seen in other current weight loss methods.

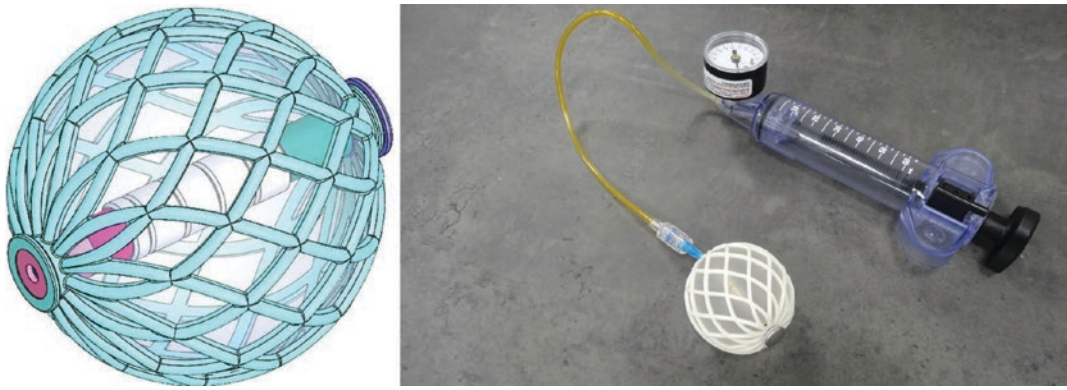

Fig. 19.3 Free floating stent balloon with internal magnet

The EMACS is advantageous over existing technology in three fundamental ways: **(I)** It is significantly smaller in size compared to existing gastric balloons (92 cc, 5.6 cm in diameter), yet large enough not to pass pyloric channel and is far less likely to cause symptoms and complications associated with chronic distention of existing balloons (750–900 cc). It is comparable in size to transpyloric shuttle device [44]. **(II)** It is used intermittently and on-demand, thereby reducing the likelihood of adaptation by the body. **(III)** The external component of the device is linked with a behavioral modification platform. Without this platform, the device is inoperable. This introduces behavioral modification as a component of treatment and can be used prior to placement of the device to select patients likely to be compliant. Furthermore, once the device has been removed after 6–12 month, patients can continue to use the behavioral platform to promote long-term behavioral modification and efficacy.

There are three major components in EMACS: an external magnet, an intragastric stent magnet device, and the platform for a patient to interact with and to monitor one's progress. This system allows the patient to manipulate the stomach intermittently and on demand, which is unlike any currently available intragastric balloon. Secondly, since the intragastric stent magnet device is controlled by the patient, it minimizes discomfort to the patient as distension only occurs when the subject feels hungry or at mealtimes. More importantly, patient control of the device allows this intragastric balloon to overcome the challenge of adaptation current balloons face. This makes the device more sustainable and because it is transient, it is less likely to cause mucosal damage. Additionally, it allows the patient to determine which part of the stomach is best manipulated, for example, the gastric body versus fundus. Lastly, the patient interaction with the platform has a significant opportunity to modify behavior. The platform introduces behavioral modification which can be used prior to placement of the device to select patients likely to be compliant. Furthermore, once the device has been removed after 6–12 month, patients can continue to use the behavioral platform to promote long-term behavioral modification and efficacy.

Since the strength required for the external magnet is quite substantial and can potentially cause injury if the user is accidentally trapped by the attraction between the strong magnet and another magnetic surface, such as steel, we have developed two design concepts for the external magnet to minimize the risks (Fig. 19.4). In the first design, the external magnet is a strong permanent magnet enclosed in a plastic case with magnetic shielding sheet embedded, except for its operating surface. The operating surface is covered by force absorbing material, such as Sorbothane®. The plastic case is designed with a variable spacer to maintain a safe distance between the external magnet and the intragastric

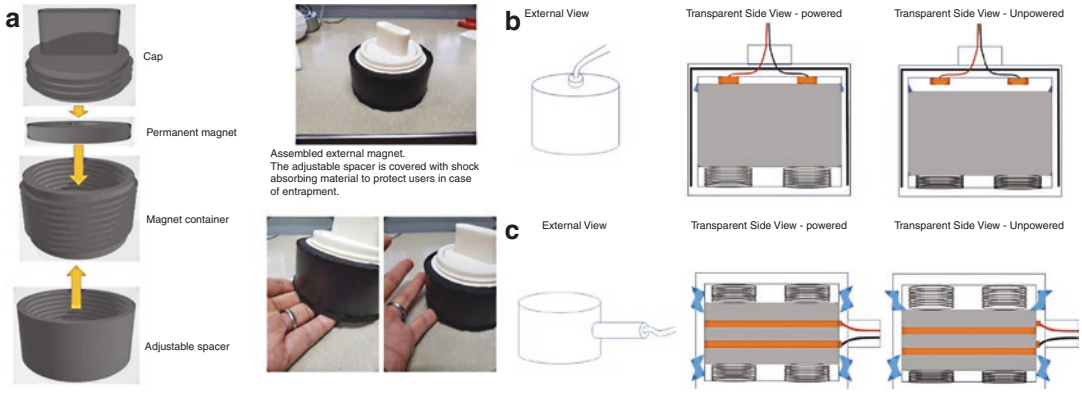

Fig. 19.4 (**a**) External magnet casing and adjustable spacer. (**b**, **c**) Designs of electromagnet housing with emergency shut-down feature for safety. The upper diagram (**b**) is a design for single pole magnet. The lower diagram (**c**) is for bipolar magnets

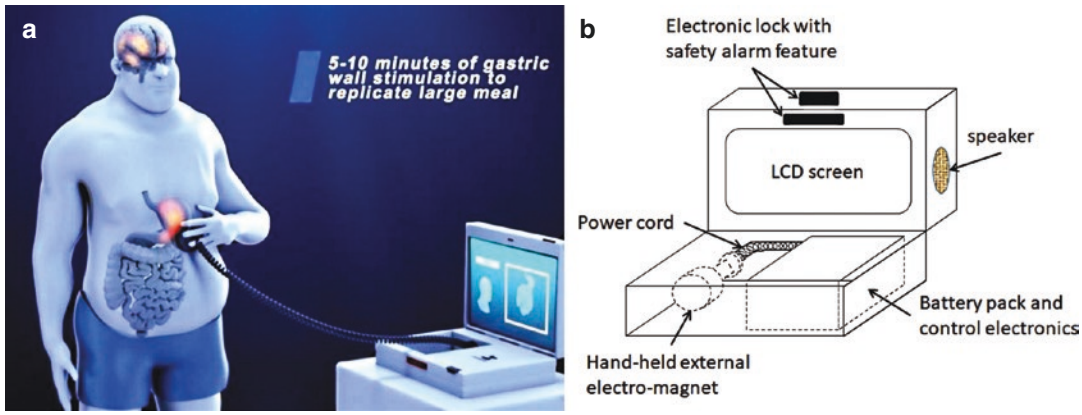

Fig. 19.5 (**a**, **b**) The magnet case that houses the EMACS platform. This diagram presents the design for housing an electromagnet. For the permanent magnet version, the battery pack may be reduced, and power cord replaced by a spiral cord to attach the magnet to the case

device, as well as with other magnetic surfaces [61]. The second version is an electromagnet. To achieve the strongest possible electromagnet with the least required electric current (to increase battery life and minimize ohmic heating), the materials used for the core of the electromagnet need to have high permeability and high saturation field. Electric metals, commonly found in high power transformers, are often used for this purpose [61]. When the electromagnet is powered, it can be equally strong as the permanent magnet if not stronger. To minimize potential operational risk, not just a layer of force absorbing material is added to the operating surface, the electromagnet is also equipped with an emergency shut-down mechanism in case of accidental entrapment. A manual reset is required to power the magnet again.

The platform would be embedded in a small magnet case, about the size of a personal computer case. The case is designed to carry and operate a handheld external magnet connected by a cord to the case for the capture and manipulation of the intragastric magnet (Fig. 19.5). The magnet case includes an LCD screen to display system information and monitor patient progress. The controller unit for the electromagnet monitors the operation time and cuts the power when

the time limit is reached (in this version of an external electromagnet). The central platform will have the ability to incorporate artificial intelligence to optimize diet, exercise, and behavioral modification and be further managed by a healthcare provider via internet connection. These added features should significantly enhance the long-term efficacy of the device.

Developmental Approach of EMACS

EMACS is currently in the prototype development and animal testing stage. The developmental process from rough sketch to prototype development and experimental design has had to consider the following:

- Historical use and safety of magnets in the GI tract [62]
- Practicality and safety of the magnetic forces required to operate the system
- Ease of endoscopic placement and removal
- Durability and functionality of the system within the GI tract
- Experimental design in appropriate animal model to test safety and explore the mechanism of action

Magnets in the GI Tract

Magnets in cattle have been used since the 1950s. Two-and-a-half- to three-inch alnico bar magnets were placed in the stomachs of cattle to control bovine traumatic gastritis [63]. In humans, magnets were first used in 1957 to safely retrieve foreign bodies from the stomach and esophagus [59]. Magnetically actuated capsule systems have been extensively studied in the literature [53, 64–67]. These systems utilize permanent magnets in a capsule system and an external magnetic field, which is used to control the capsule locomotion [53]. The development of magnet-assisted capsule endoscopy (MACE) systems occurred in 2009, with additional experiments in 2010 and 2013. The development of magnetic capsule manipulation allows capsules to be steered so areas of the gastrointestinal tract that are being passed too quickly or large cavities can be thoroughly examined [68]. These trials include the given image system, which creates a maximum magnetic force between capsule and magnet of 256 g/cm^2 (25.1 kPa). The Olympus and Siemens system, developed in 2010, uses a magnetic field of up to 200 mT, and a MicroCam-Navi, which has a pressure of 30.3 kPa [66, 67]. These studies note that magnetic strength drops exponentially with distance, and that the external magnet can initiate capsule movement on a vertical plane at ~8cm [69]. The 2013 trial consisted of the use of a Microcam-Navi device on twenty-six subjects, a median procedure time of 24 minutes, with five positions requiring the internal magnet be held in a stagnant position by the external magnet for one minute [66]. In these studies, no serious adverse effects were reported. Nor were there reports of any evidence of mucosal injury.

Additional magnetic devices include the Gabriel Blue Tube and the Levita Magnetic Surgical System, both of which are FDA approved [70]. The Gabriel Blue Tube consists of three handheld N42 magnets: 7, 5, and 3 lbs. We calculated the resultant gastric mucosa pressures to be up to 150 kPa [71, 72]. There have been no reports of mucosal damage in published trials or in postmarketing. The Levita Magnetic Surgical System utilizes a trocar with a magnetic detachable tip and a large magnet controller that is maneuvered across the abdomen, which applies pressures of up to 250 kPa based on a standard N42 magnet [73]. Frequently when magnets are used in devices, the manufacturer focuses on the strength of the magnetic field. When two magnets are used in a system, it is imperative that the magnetic force between the two magnets and the resultant pressure on any tissue is known.

Practicality and Safety of the Magnetic Forces Required to Operate the System

Surprisingly, there was scant information in the literature regarding the variability of the distance between the skin and the stomach in human sub-

jects. Given that the size of the introducer needle for percutaneous endoscopic gastrostomy (PEG) placement is the same for all subjects, we suspected that there would be small variability across a wide BMI range.

Trans-gastric magnetic capture is an existing and utilized concept. In the development of Microcam-Navi, computed tomography (CT) was undertaken and estimated the skin surface to the proximal and distal stomach to be 16.5cm and 9.0cm. These measurements were taken from the skin to the center of the distal and proximal stomach, not to the stomach mucosa.

Using Human Patients, Our Team Determined

Variability of the Abdominal Wall Over a Wide Range of BMI

To create our device, we needed to determine the distance from the skin surface to the inner gastric mucosa of the antrum and fundus to determine a range of operation of the trans-gastric magnetic device. We analyzed 114 CT scans of the abdomen, with and without standard contrast to assess fundus and antrum measurements with regard to BMI, contrast status, and sex. The patient characteristics were taken from medical charts. Continuous measures were reported as means and standard deviations (SD) or medians and interquartile ranges (IQR). Categorical measures were reported as frequencies and percentages. Spearman's rank order correlation was used to assess the relationship between BMI and fundus and antrum measurements. The Kruskal–Wallis test was used to compare fundus and antrum measurements by BMI categories. The Mann–Whitney U test was used to compare fundus and antrum measurements by contrast status and sex. A p-value < 0.05 was used to define statistical significance for all tests conducted. SAS software version 9.4 was used for all analyses.

Among the sample of patients, the mean age was 50 years, 66% were female, the median BMI measurement was 29.50 kg/m^2, the median fundus measurement was 59.80 mm, and the median antrum measurement was 37.00 mm (Table 19.1). A statistically significant correlation was shown between BMI and both fundus and antrum measurements (both p < 0.0001, Table 19.2). There was a moderately positive relationship between BMI and fundus measurement (rho=0.48) and BMI and antrum measurement (rho=0.58). When making comparisons by BMI categories, both the fundus measurement and antrum measurement were significantly different by category (both p<0.0001, Table 19.3). Post-hoc comparisons revealed that the fundus measurement was significantly different between the ≤30 kg/m^{2}and the

Table 19.1 Descriptive characteristics of patients (N=113 patients, N=114 procedures[a])

Characteristic	
Age (years)	
Mean (±SD)	50.01 (±18.48)
Sex, n (%)	
Male	38 (33.63)
Female	75 (66.37)
Contrast, n (%)	
Yes	53 (46.49)
No	61 (53.51)
BMI (kg/m^2)	
Median (IQR)	29.50 (25.00, 35.00)
BMI Categories, n (%)	
≤30	65 (57.02)
31–39	36 (31.58)
≥40	13 (11.40)
Fundus (mm)	
Median (IQR)	59.80 (36.50, 95.00)
Antrum (mm)	
Median (IQR)	37.00 (28.10, 47.10)

IQR interquartile range, *SD* standard deviation
[a]Note: There were 113 total patients but 114 procedures because one patient had two procedures. N = 113 for age and sex results; N = 114 for contrast, BMI, fundus, and antrum results

Table 19.2 Correlation between BMI and fundus and antrum measurements (N = 114)

	Spearman's rho	p-value[a]
BMI (kg/m^2) and fundus (mm)	0.48	<0.0001
BMI (kg/m^2) and antrum (mm)	0.58	<0.0001

[a]p-value derived from the Spearman's rank order correlation test

Table 19.3 Comparison of fundus and antrum measurements by BMI categories (*N*=114)

	BMI ≤ 30 kg/m² *n* = 65	BMI 31–39 kg/m² *n* = 36	BMI ≥ 40 kg/m² *n* = 13	*p*-value[a]
Fundus (mm)				
Median (IQR)	47.80 (32.00, 78.90)	60.90 (46.85, 92.70)	115.40 (110.30, 123.00)	<0.0001[b]
Antrum (mm)				
Median (IQR)	33.00 (25.00, 39.50)	38.70 (30.30, 48.35)	67.40 (52.90, 82.50)	<0.0001[c]

IQR interquartile range

[a]*p*-value derived by the Kruskal-Wallis test

[b]Post-hoc tests indicate the following pairwise comparisons are significant at the 0.05 level:
BMI ≤30 kg/m²and BMI ≥40 kg/m²
BMI 31–39 kg/m²and BMI ≥40 kg/m²

[c]Post-hoc tests indicate the following pairwise comparisons are significant at the 0.05 level:
BMI ≤30 kg/m²and BMI 31–39 kg/m²
BMI ≤30 kg/m²and BMI ≥40 kg/m²
BMI 31–39 kg/m²and BMI ≥40 kg/m²

≥40 kg/m²groups, and the 31–39 kg/m²and the ≥40 kg/m²groups. It was not significantly different between the ≤30 kg/m²and BMI 31–39 kg/m²groups. Post-hoc comparisons revealed that the antrum measurement was significantly different between the ≤30 kg/m²and the 31–39 kg/m²groups, the ≤30 kg/m²and the ≥40 kg/m²groups, and the 31–39 kg/m²and the ≥40 kg/m²groups.

Fundus and antrum measurements were compared by sex for each BMI category (Table 19.4). There were no significant differences in measurements between males and females, except for the antrum measurement in the 31–39 kg/m² category (36.30 mm vs. 44.20 mm, p=0.028). Antrum measurements were also compared by sex for patients who had a BMI between 20 and 45 kg/m², and there were no significant differences between males and females (Table 19.5).

There was a significant difference in fundus and antrum measurements by contrast status (Table 19.6). The median fundus measurement for those with contrast was smaller than the median fundus measurement for those without contrast (42.60 mm vs. 89.60 mm, p<0.0001). The median antrum measurement was smaller for those with contrast compared to those without contrast (33.00 mm vs. 39.50 mm, p=0.033).

In summary, despite the expected positive correlation between the measured distance from the stomach to the skin surface and BMI, we found that the change in distance is small in the antrum, but not in the fundus, across a wide BMI range with or without contrast. This provides an ideal location for capture of intragastric devices that use trans-gastric manipulation due to the short and stable distance from the internal gastric

Table 19.4 Comparison of fundus and antrum measurements by sex per BMI category (*N* = 114)

	BMI ≤ 30 kg/m²		
	Male *n* = 24	**Female *n* = 41**	***p*-value[a]**
Fundus (mm)			
Median (IQR)	67.45 (35.50, 82.60)	44.30 (30.30, 60.50)	0.15
Antrum (mm)			
Median (IQR)	31.75 (26.70, 41.50)	34.10 (22.80, 38.90)	0.57
	BMI 31–39 kg/m²		
	Male *n*=12	**Female *n*=24**	***p*-value[a]**
Fundus (mm)			
Median (IQR)	60.35 (28.25, 99.25)	60.90 (53.15, 86.70)	0.61
Antrum (mm)			
Median (IQR)	36.30 (22.90, 38.70)	44.20 (31.40, 52.05)	0.028
	BMI ≥ 40 kg/m²		
	Male *n*=2	**Female *n*=11**	***p*-value[a]**
Fundus (mm)			
Median (IQR)	142.15 (137.80 146.50)	113.60 (96.50, 122.90)	0.060
Antrum (mm)			
Median (IQR)	85.00 (84.00, 86.00)	56.70 (52.60, 71.80)	0.12

IQR interquartile range

[a]*p*-value derived by the Mann-Whitney U test

mucosa to the abdominal wall [74]. Subsequent to the capture of the intragastric device, the body and fundus would be readily amenable to stimulation and distension.

Table 19.5 Comparison of antrum measurement by sex for BMI 20–45 kg/m^2(*N*=103)

	Male *n*=36	Female *n*=67	*p*-value[a]
Antrum (mm)			
Median (IQR)	34.65 (26.70, 41.20)	38.60 (31.30, 49.00)	0.058

IQR interquartile range
[a]*p*-value derived by the Mann-Whitney U test

Table 19.6 Comparison of fundus and antrum measurements by contrast categories (*N*=114)

	Contrast *n*=53	No Contrast *n*=61	*p*-value[a]
Fundus (mm)			
Median (IQR)	42.60 (30.40, 50.20)	89.60 (71.30, 103.80)	<0.0001
Antrum (mm)			
Median (IQR)	33.00 (23.50, 42.20)	39.50 (31.40, 51.50)	0.0033

IQR interquartile range
[a]*p*-value derived by the Mann-Whitney U test

Calculated Pressure Ranges That Would Be Generated by the Proposed Internal and External Magnets

To identify and optimize the configuration in which the external magnet would produce enough pulling force on the internal magnetic intragastric device, we employed a theoretical model called the Gilbert model (Fig. 19.6) to calculate the expected magnetic force between the two over a range of distance from 2 to 8 cm with 0.5 cm interval. The dimension of the internal device is a cylinder of 9.5mm (OD) x 19mm (length) and is similar to a PillCam device. The size of the external magnet is determined by two criteria. One is to produce a pulling force ~2 *N* (equivalent to the weight of roughly 200 g) at 5 cm distance, and the other is to be as lightweight as possible. Using the physical parameters (surface magnetization, mass density, etc.) of N42 grade magnets for both the internal and external magnet, the Gilbert model calculations suggest the external magnet to be a disk of 6.35 cm (OD) x 1.27 cm (thickness), which is about the lightest weight possible to produce ~2 *N* of force. Bench tests were then conducted to measure the magnetic force between the two magnets by attaching the internal magnet to a force sensor while being pulled by the external

$$F_m = \frac{1}{4\pi\mu_0}\left(\int_{A_1^+}\int_{A_2^+}\frac{q_{m,1^+}\,q_{m,2^+}}{|r_{1^+2^+}|^2}dA_2^+\,dA_1^+ + \int_{A_1^-}\int_{A_2^+}\frac{q_{m,1^-}\,q_{m,2^+}}{|r_{1^-2^+}|^2}dA_2^+\,dA_1^- + \int_{A_1^+}\int_{A_2^-}\frac{q_{m,1^+}\,q_{m,2^-}}{|r_{1^+2^-}|^2}dA_2^-\,dA_1^+ + \int_{A_1^-}\int_{A_2^-}\frac{q_{m,1^-}\,q_{m,2^-}}{|r_{1^-2^-}|^2}dA_2^-\,dA_1^-\right).$$

Fig. 19.6 Gilbert Model equation integrates for the cylindrical coordinate system, where + denotes the north pole face, − denotes the south pole face, index 1 indicates the hand-held magnet, index 2 indicates the magnetic pill, and *A* denotes surface integration over the area of the pole faces

magnet at ½-cm intervals for an 8-cm distance. Reliability of the Gilbert model calculation was affirmed by the bench test data and the greatest difference between the two is less than 15%. Given the nonideal magnetization of the N42 magnets and the uncertainty in distance measurements, this level of discrepancy is expected.

Once the magnetic force profile between 2-cm and 8-cm distance was established, the induced pressure was determined by first finding the contact area between the intragastric device and the gastric mucosa. Since the internal magnet is located at the center of an intragastric balloon of diameter 6.5 cm, the area of contact the balloon makes with the gastric mucosa is similar to a circle with diameter ~2.5 cm. The magnet-induced pressure is then calculated by dividing the above-measured force by this contact area (P = F/A, the definition of pressure) [75].

Compare the Calculated Pressure Range to Known Gastric Wall Pressure Profiles Found in Endoscopy, Surgery, or With Other Medical Equipment in Clinical Use

In humans, vomiting can produce pressures of 38.65 kPa. In animal studies using rats, pressures of 50 kPa have been reported as safe on thigh muscle tissue after compressive loading. Peg tube bumpers, when tight, are reported to cause gastric mucosa ulcerations after 7 days, and when measured in actual patients by us had acute pressures from 10 to 27 kPa. Similarly, in laboratory tissue models compressed by peg tube bumpers, we were able to produce pressures of 30, 70, and 248 kPa with tissue thicknesses of 0.8, 1.05, and 1.3 cm, respectively. Pressures of 19.3–26.2 kPa were used with the Olympus CV 160 Evis Exera to open the stomach during endoscopy (Fig. 19.7).

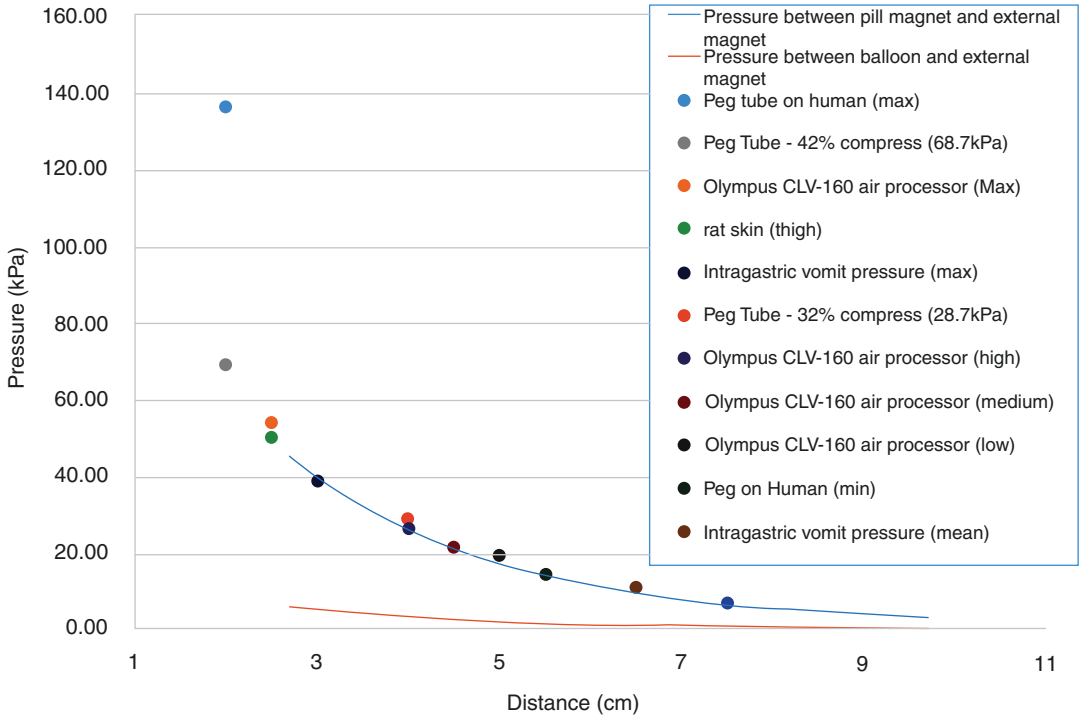

Fig. 19.7 Measured magnet induced pressure between handheld magnet (63.5mm x 50.8mm) and internal magnet (pill magnet 9.5mmx19mm) versus distance as compared to historical and experimental trans-gastric pressures. The pressure between handheld external magnet and a magnet-containing balloon is also shown for comparison. Note the cutoff at 3 cm which represents the shortest hypothetical distance between the internal magnet positioned inside the balloon and the skin surface

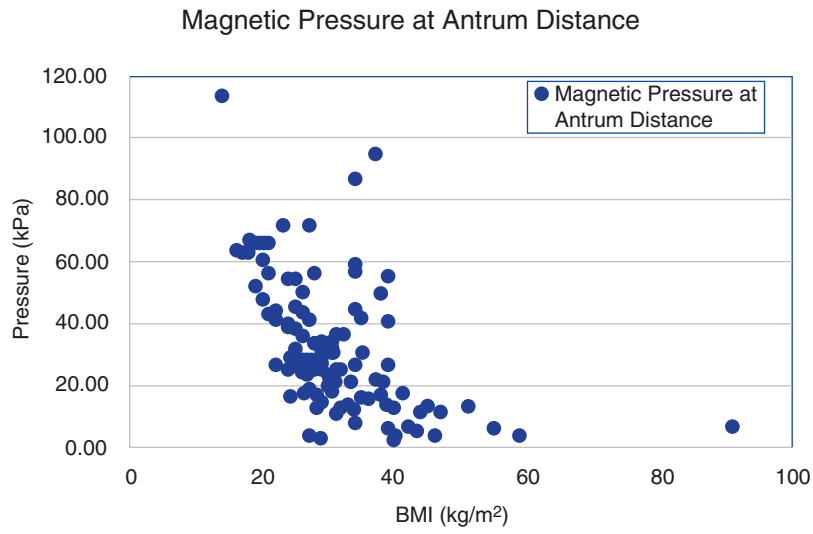

Fig. 19.8 Expected magnetic force relative to distance of the antrum/fundus to abdominal skin surface relative to BMI in 114 sequential patients, with a wide BMI range, who had undergone CT imaging with measured shortest skin to antral mucosa and skin to fundal mucosa

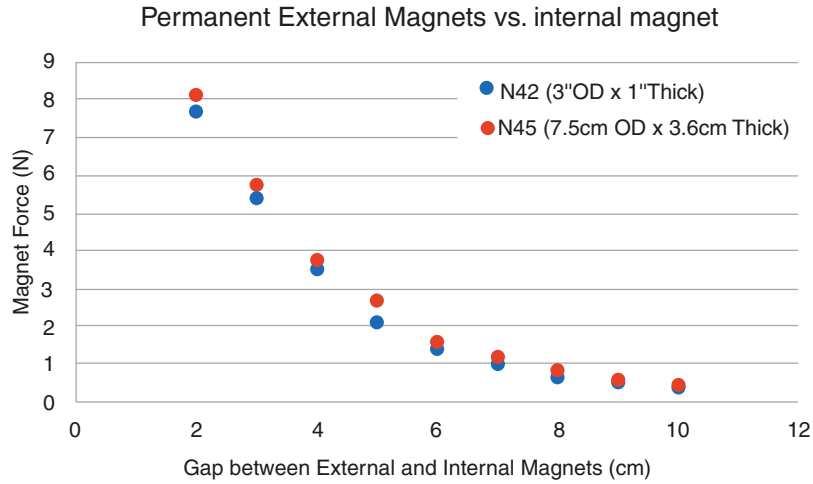

Fig. 19.9 The force between the magnetic intragastric balloon and two similar external magnets. The balloon can be moved and captured by the N42 external magnet at a distance of more 10 cm away from the external magnet

Also, recent publications show pressures of 200–600 kPa with graspers on the gastric wall during laparoscopic surgery [75–77].

Using Gilbert formula and hypothetical magnet sizes (cylinder of 3.1 cm in diameter and 19mm in length and external magnet is a disk of 6.35cm in diameter and 1.27cm in thickness), we calculated the hypothetical gastric wall pressures between the two magnets in the 114 patients in which we had CT data (Fig. 19.8). The size and strength of the magnets were calculated such that they conformed to anatomical use. As can be seen, there is a wide range of operability of 20–55.

Due to the large contact area between the intragastric balloon and the gastric mucosa, it allows the use of even stronger magnets than currently proposed to generate larger forces for capture if needed for patients with larger BMI, but minimal surface pressures < 20kPa. Our current prototype consists of an internal magnet 3.1 cm mm in diameter and 19 mm long and the external magnet is 3” in diameter and 1” thick. Capture readily occurs at less than 16 cm (Fig. 19.9). The pressure profile for this external magnet and an additional larger magnet are shown in the attached graph (Fig. 19.10).

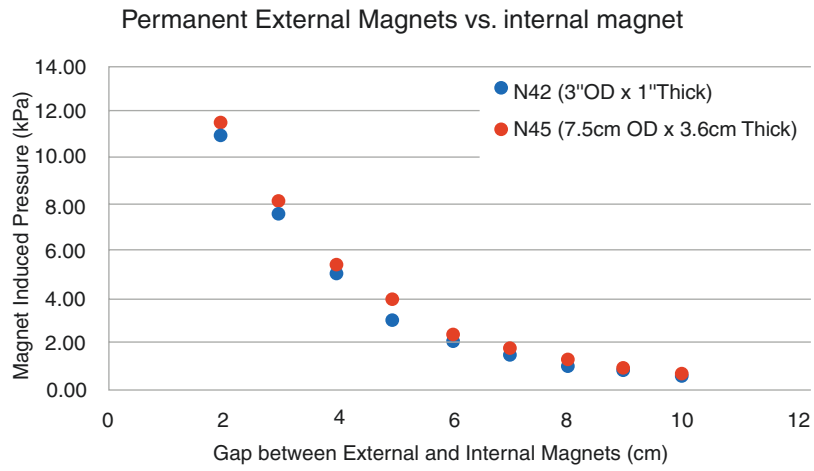

Fig. 19.10 The pressures induced by the force between the magnetic intragastric balloon and two similar external magnets, respective, based on the data in Fig. 19.9

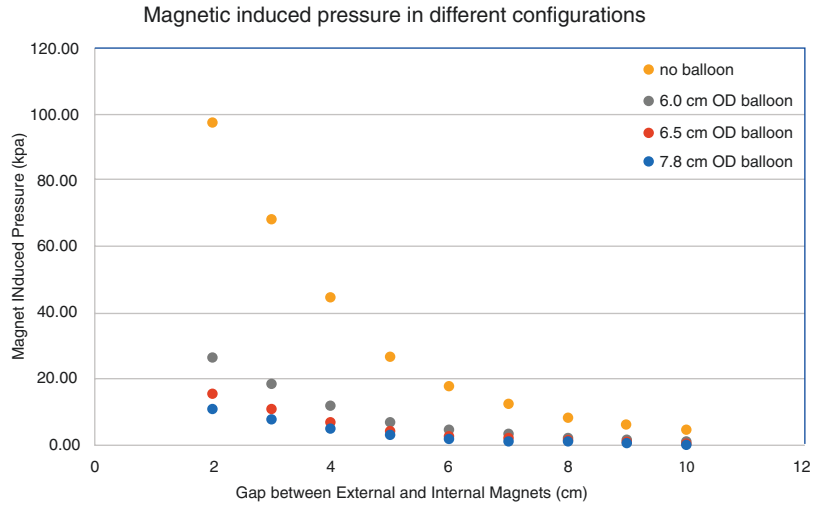

Fig. 19.11 Gap between internal and external magnets vs pressure

Our balloon stent currently is at a diameter of 6.5cm. The magnetic force and pressures generated are represented in the diagrams below depending on the size of the sphere (Fig. 19.11). It should be noted that the minimum distance between gastric mucosa and abdominal wall surface is estimated to be ~3cm [73, 78].

Endoscopic Placement and Removal

The intragastric portion of the device has to be delivered and removed relatively easily and remain intact in the gastric environment for 6 months or longer. The intragastric device contains the stent, a balloon, and a shaft on which the internal magnet is housed. Prior to deployment, the balloon is completely deflated, and the stent and its delivery components are wrapped in a cover sheet with a diameter of 18 cm so that it can easily pass the esophagus into the stomach. The device is inserted endoscopically through the esophagus with the help of a guidewire and an option to use an overtube, if needed. Also accompanying the guidewire is an inflation tube that is inserted into the device through a check valve. When the device enters the stomach, the device will first be released from the sheet cover, followed by removal of the guidewire. Our current prototypes have options of bioabsorbable cover sheet or traditional retrievable cover sheet. Once the balloon is free from the cover sheet, it will be

inflated to expand the stent to the full size followed by the removal of the inflation tube. The placement of the intragastric device is now complete and the endoscope will be removed. The whole procedure is under endoscopic monitoring to ensure proper placement of the device.

To remove the intragastric device, an endoscope is placed. The balloon must be deflated first. Forceps are inserted through the endoscope under direct vision and the balloon is captured, punctured, and air is released. The deflation could be enhanced with the aid of a suction catheter and a pump. When the balloon is deflated, a collar on the center shaft will be accessible for placement of a suture snare to assist in removal of the device. Then the device will be pulled out of the stomach by pulling the endoscope, suture wire, and the deflated stent balloon as a system. Since the balloon is punctured and no longer pressurized, as the device exits the stomach and enters the esophagus, it will collapse and conform to the size of the esophagus. Alternatively, an overtube can also be used in this procedure to assist removal.

Durability and Functionality of the System Within the GI Tract

Since the intragastric device is intended to stay in the stomach for 6 months to one year, the materials must be durable so that the integrity and the functionality of the device can be maintained at all times. To endure the hostile environment in the stomach, with acid and movements, the material used to make the stent and balloon must be not only biocompatible, but also acid-resistant and shear-resistant. We choose to use silicon for this application due to prior approval for usage in similar conditions. It is also flexible enough to endure substantial shape change during implementation (inflated), in-operation (squeezed and compressed), and removal (deflated).

The internal magnet is slid on a sliding tube that goes through the center of the balloon and stent. The tube is joined to the stent/balloon structure on both ends with check valves allowing the guidewire and inflation tube to go through. The sliding movement of the internal magnet is limited to the center third of the tube. This arrangement is to allow force, when attracted by the external magnet, to be more uniformly distributed over a bigger contact area between the intragastric device and the esophageal surface, instead of concentrated at the check valve. The stent frame can be broken apart with endoscopic tools if needed. This will safeguard against inadvertent balloon rupture or deflation with potential bezoar formation.

Animal Studies

It has been interesting that most interventions in the field of bariatric surgery or endoscopy have been made without detailed attention to underlying potential mechanism of action. The potential mechanisms for neurohormonal pathways that could be affected and utilized by EMACS have been discussed earlier. We have proposed the following animal protocol that would not only establish the safety of the device in an animal model but at least provide insight into possible mechanism of action. We are also aware that the cornerstone of our device, that is, incorporation of behavior modification to change eating habits, will not be applicable in an animal model, especially swine. However, the swine stomach is similar in size and shape to a human stomach. The pig anatomy makes it ideal for magnetic capture and the distance from skin to gastric wall is ~5 cm [57]. Pigs in the 20–50 kg range have been used in previous bariatric studies [58]. Mini pigs will be used to determine feasibility of placement, durability, and removal of the device. Also, the mini pigs will be used to determine the proposed efficacy of the device by monitoring the effect of the device on pig growth, weight, and the impact on GI hormones involved in satiety. Mini pigs weighing 20 kg at the onset of the study on a feed to grow diet normally weigh 50 kg after 6 months. The rationale for mini pigs is shorter stature and shorter distance between their abdomen and the ground, allowing for the use of external magnets at the bottom of a special cage (Fig. 19.12).

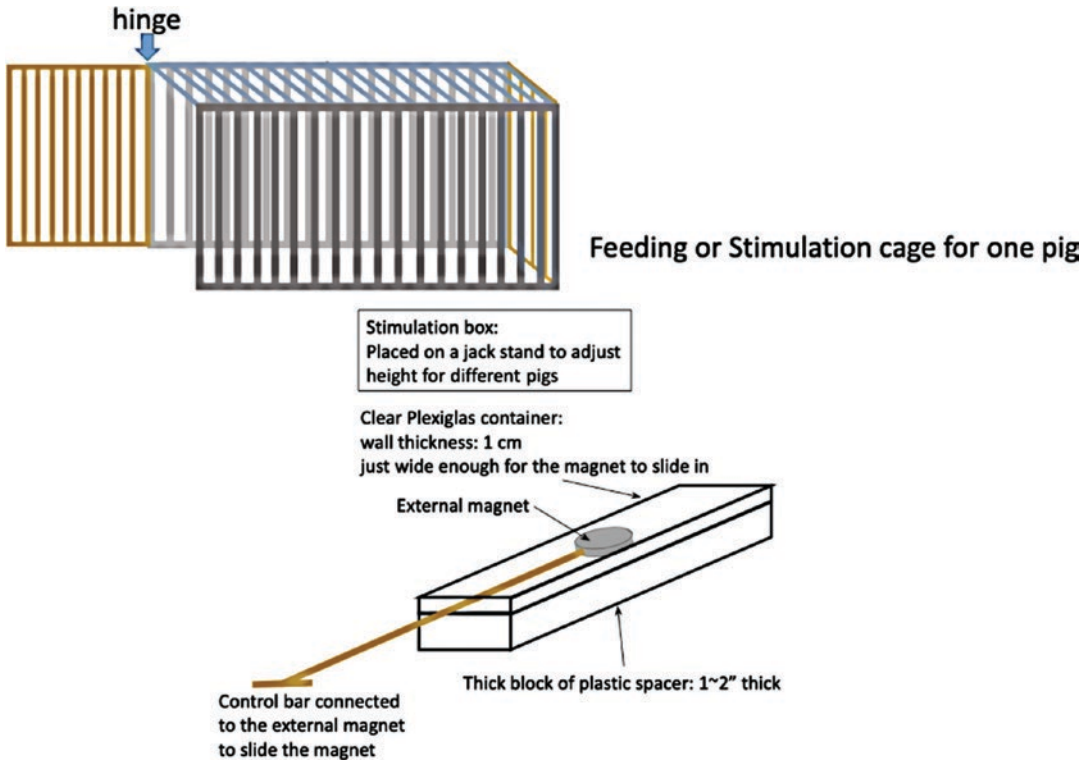

Fig. 19.12 Animal cage to allow for the use of external magnets during animal studies

Initially, two pigs weighing 20kg and 50kg, respectively, will be used. Technical aspects related to sedation, anesthesia, blood draw, removal, and magnetic capture will be tested and practiced on these two pigs, ahead of planned animal studies. Twelve pigs, six males and six females, weighing 20kg will be housed in a group stall.

1. Six male and six female mini pigs will have anatomical measurements including weight, height, and distance of the abdomen to ground. Lab values (CBC, chemistry, and gut peptides) will be obtained. The device will be placed endoscopically, expanded, and released in the stomach in eight pigs (four male), with four non device pigs serving as controls who will have sham endoscopy. The pigs will be housed together (flooring will be elevated such that it will minimize the risk of pica) and will only have access to water.
2. At specific hours each day, individual pigs will be taken to special individual experimental cages (Fig. 19.12) where they will be fed twice daily. The cage is designed so the pig is relatively immobile. The magnetic simulation will be done by the technician using an external magnet under a clear plexiglass floor. The size, height, and distance of the external magnet will be adjusted according to pig size to simulate magnetic pressures comparable to a human subject by rubbing an external magnet on the surface of the abdomen. Different sized cages corresponding to different time intervals in the study will be used.
3. Each month baseline feeding duration in pigs will be measured and is expected to be 9–11 minutes [4, 60]. Five minutes of gastric stimulation simultaneous with normal feeding time will be performed at the onset of feeding alternating with the midpoint of feeding in a counterbalanced crossover fashion with a

switch at 3 months. The technician will ensure that the magnet movement corresponds to the anatomical element of the pig stomach.

4. Food consumption will be measured by the MBRose individual feed Intake monitor [61], and the pig will be returned to the group stall.
5. The magnet will be detected weekly in the experimental group via a metal detector. If not detected, the pig will undergo further imaging.
6. At 1, 3, and 6 months, the pigs will undergo baseline fasting peptide measurement and then upper endoscopy for visualization of the GI tract with assessment, by biopsy (H&E staining) of any damage to the esophagus and stomach.
7. After endoscopic examination is completed, a 200-cc liquid meal via an OG tube while the pig is intubated is given and a 5-minute magnetic stimulation will be given by a handheld magnet. Peptide levels will be measured at 0, 15, 30, and 60 minutes.
8. Control pigs will have identical protocols without the magnetic stimulation using a simulated nonmagnetic device (placebo). At 6 months, the device is collapsed by air suction and removed endoscopically.
9. Two weeks after the last endoscopy, the pigs will be euthanized per IACUC guidelines and gross and microscopic (H&E) visualization of the stomach will be done.

Conclusion and Future

Obesity and its complications are now the leading cause of morbidity and mortality worldwide. It is unlikely that the food industry will take a meaningful and active role in combating obesity anytime soon. New innovations are required to help modify human behavior with respect to control of appetite and food. Magnets can provide a safe and effective way to simulate the pathways that are activated upon eating in an effort to provide the patients a tool to help reinforce behavior modification. The proposed device, EMACS, has been designed to accommodate this need and in 3 years.

References

1. Begley S. Fat and getting fatter: U.S. obesity rates to soar by 2030. Reuters. Published 18 Sept 2012. https://www.reuters.com/article/us-obesity-us/fat-and-getting-fatter-u-s-obesity-rates-to-soar-by-2030-idUSBRE88H0RA20120918.
2. Hruby A, Hu FB. The epidemiology of obesity: a big picture. Pharm Econ. 2015;33(7):673–89. https://doi.org/10.1007/s40273-014-0243-x.
3. Wang Y, Beydoun MA, Liang L, Caballero B, Kumanyika SK. Will all Americans become overweight or obese? estimating the progression and cost of the US obesity epidemic. Obesity (Silver Spring). 2008;16(10):2323–30. https://doi.org/10.1038/oby.2008.351.
4. Kentish SJ, O'Donnell TA, Frisby CL, Li H, Wittert GA, Page AJ. Altered gastric vagal mechanosensitivity in diet-induced obesity persists on return to normalchow and is accompanied by increased food intake. Int J Obes 2005. 2014;38(5):636–42. https://doi.org/10.1038/ijo.2013.138.
5. Abdelaal M, le Roux CW, Docherty NG. Morbidity and mortality associated with obesity. Ann Transl Med. 2017;5(7) https://doi.org/10.21037/atm.2017.03.107.
6. Roth J, Qiang X, Marbán SL, Redelt H, Lowell BC. The obesity pandemic: where have we been and where are we going? Obes Res. 2004;12(Suppl 2):88S–101S. https://doi.org/10.1038/oby.2004.273.
7. Mohammed MA, Anwar R, Mansour AH, Elmasry E, Othman G. Effects of intragastric balloon versus conservative therapy on appetite regulatory hormones in obese subjects. Trends Med Res. 2014;9(2):58–80. https://doi.org/10.3923/tmr.2014.58.80.
8. Meldrum DR, Morris MA, Gambone JC. Obesity pandemic: causes, consequences, and solutions-but do we have the will? Fertil Steril. 2017;107(4):833–9. https://doi.org/10.1016/j.fertnstert.2017.02.104.
9. Swinburn BA. Obesity prevention: the role of policies, laws and regulations. Aust New Zealand Health Policy. 2008;5(1):12. https://doi.org/10.1186/1743-8462-5-12.
10. Davy B, Jahren H. New markers of dietary added sugar intake. Current Opinion in Clinical Nutrition and Metabolic Care. 2016;19:1. https://doi.org/10.1097/MCO.0000000000000287.
11. Christakis NA, Fowler JH. The spread of obesity in a large social network over 32 years. N Engl J Med. 2007;357(4):370–9. https://doi.org/10.1056/NEJMsa066082.
12. Kral TVE, Roe LS, Rolls BJ. Combined effects of energy density and portion size on energy intake in women. Am J Clin Nutr. 2004;79(6):962–8. https://doi.org/10.1093/ajcn/79.6.962.
13. Milanski M, Arruda AP, Coope A, et al. Inhibition of hypothalamic inflammation reverses diet-induced insulin resistance in the liver. Diabetes. 2012;61(6):1455–62. https://doi.org/10.2337/db11-0390.

14. Milanski M, Degasperi G, Coope A, et al. Saturated fatty acids produce an inflammatory response predominantly through the activation of TLR4 signaling in hypothalamus: implications for the pathogenesis of obesity. J Neurosci. 2009;29(2):359–70. https://doi.org/10.1523/JNEUROSCI.2760-08.2009.
15. De Souza CT, Araujo EP, Bordin S, et al. Consumption of a fat-rich diet activates a proinflammatory response and induces insulin resistance in the hypothalamus. Endocrinology. 2005;146(10):4192–9. https://doi.org/10.1210/en.2004-1520.
16. Simpson KA, Bloom SR. Appetite and Hedonism: Gut Hormones and the Brain. Endocrinology and Metabolism Clinics of North America. 2010;39(4):729–43. https://doi.org/10.1016/j.ecl.2010.08.001.
17. Cummings DE, Overduin J. Gastrointestinal regulation of food intake. J Clin Invest. 2007;117(1):13–23. https://doi.org/10.1172/JCI30227.
18. Wang G-J, Tomasi D, Backus W, et al. Gastric distention activates satiety circuitry in the human brain. NeuroImage. 2008;39(4):1824–31. https://doi.org/10.1016/j.neuroimage.2007.11.008.
19. Ly HG, Dupont P, Van Laere K, Depoortere I, Tack J, Van Oudenhove L. Differential brain responses to gradual intragastric nutrient infusion and gastric balloon distension: A role for gut peptides? NeuroImage. 2017;144:101–12. https://doi.org/10.1016/j.neuroimage.2016.09.032.
20. Raynor HA, Champagne CM. Position of the academy of nutrition and dietetics: interventions for the treatment of overweight and obesity in adults. J Acad Nutr Diet. 2016;116(1):129–47. https://doi.org/10.1016/j.jand.2015.10.031.
21. Berthoud H-R, Münzberg H, Morrison CD. Blaming the brain for obesity: Integration of hedonic and homeostatic mechanisms. Gastroenterology. 2017;152(7):1728–38. https://doi.org/10.1053/j.gastro.2016.12.050.
22. Ritter RC. Gastrointestinal mechanisms of satiation for food. Physiology & Behavior. 2004;81(2):249–73. https://doi.org/10.1016/j.physbeh.2004.02.012.
23. Stice E, Spoor S, Bohon C, Veldhuizen MG, Small DM. Relation of reward from food intake and anticipated food intake to obesity: a functional magnetic resonance imaging study. J Abnorm Psychol. 2008;117(4):924–35. https://doi.org/10.1037/a0013600.
24. Geiger BM, Behr GG, Frank LE, et al. Evidence for defective mesolimbic dopamine exocytosis in obesity-prone rats. FASEB J. 2008;22(8):2740–6. https://doi.org/10.1096/fj.08-110759.
25. Volkow ND, Wang G-J, Telang F, et al. Low dopamine striatal D2 receptors are associated with prefrontal metabolism in obese subjects: possible contributing factors. Neuroimage. 2008;42(4):1537–43. https://doi.org/10.1016/j.neuroimage.2008.06.002.
26. Dixon JB, Lambert EA, Lambert GW. Neuroendocrine adaptations to bariatric surgery. Mol Cell Endocrinol. 2015;418(Pt 2):143–52. https://doi.org/10.1016/j.mce.2015.05.033.
27. Hargrave SL, Kinzig KP. Repeated gastric distension alters food intake and neuroendocrine profiles in rats. Physiol Behav. 2012;105(4):975–81. https://doi.org/10.1016/j.physbeh.2011.11.006.
28. Woods SC, D'Alessio DA. Central control of body weight and appetite. J Clin Endocrinol Metab. 2008;93(11 Suppl 1):S37–50. https://doi.org/10.1210/jc.2008-1630.
29. Maljaars J, Peters HPF, Masclee AM. Review article: The gastrointestinal tract: neuroendocrine regulation of satiety and food intake. Aliment Pharmacol Ther. 2007;26(Suppl 2):241–50. https://doi.org/10.1111/j.1365-2036.2007.03550.x.
30. Lepionka L, Malbert CH, Laplace JP. Proximal gastric distension modifies ingestion rate in pigs. Reprod Nutr Dev. 1997;37(4):449–57. https://doi.org/10.1051/rnd:19970406.
31. Pappas TN, Melendez RL, Debas HT. Gastric distension is a physiologic satiety signal in the dog. Digest Dis Sci. 1989;34(10):1489–93. https://doi.org/10.1007/BF01537098.
32. Lepionka L, Malbert CH. Perprandial changes in gastric wall tension control ingestion in pigs. Reprod Nutr Dev. 1997;37(3):351–1. https://doi.org/10.1051/rnd:19970341.
33. Oesch S, Rüegg C, Fischer B, Degen L, Beglinger C. Effect of gastric distension prior to eating on food intake and feelings of satiety in humans. Physiology & Behavior. 2006;87(5):903–10. https://doi.org/10.1016/j.physbeh.2006.02.003.
34. Geliebter A. Gastric distension and gastric capacity in relation to food intake in humans. Physiology & Behavior. 1988;44(4–5):665–8. https://doi.org/10.1016/0031-9384(88)90333-2.
35. Stephan E, Pardo JV, Faris PL, et al. Functional neuroimaging of gastric distention. J Gastrointest Surg. 2003;7(6):740–9. https://doi.org/10.1016/s1091-255x(03)00071-4.
36. Konturek SJ, Konturek JW, Pawlik T, Brzozowki T. Brain-gut axis and its role in the control of food intake. J Physiol Pharmacol. 2004 Mar;55(1 Pt 2):137–54.
37. Oudenhove LV, Vandenberghe J, Dupont P, et al. Cortical deactivations during gastric fundus distension in health: visceral pain-specific response or attenuation of 'default mode' brain function? A H215O-PET study. Neurogastroenterology & Motility. 2009;21(3):259–71. https://doi.org/10.1111/j.1365-2982.2008.01196.x.
38. Geeraerts B, Oudenhove LV, Dupont P, et al. Different regional brain activity during physiological gastric distension compared to balloon distension: a H215O-PET study. Neurogastroenterology & Motility. 2011;23(6):533–e203. https://doi.org/10.1111/j.1365-2982.2010.01642.x.
39. Vandenbergh J, DuPont P, Fischler B, et al. Regional brain activation during proximal stomach distention in humans: A positron emission tomography study. Gastroenterology. 2005;128(3):564–73. https://doi.org/10.1053/j.gastro.2004.11.054.

40. Delzenne N, Blundell J, Brouns F, et al. Gastrointestinal targets of appetite regulation in humans. Obesity Reviews. 2010;11(3):234–50. https://doi.org/10.1111/j.1467-789X.2009.00707.x.
41. Steinert RE, Meyer-Gerspach AC, Beglinger C. The role of the stomach in the control of appetite and the secretion of satiation peptides. American Journal of Physiology-Endocrinology and Metabolism. 2012;302(6):E666–73. https://doi.org/10.1152/ajpendo.00457.2011.
42. Share I, Martyniuk E, Grossman MI. Effect of Prolonged Intragastric Feeding on Oral Food Intake in Dogs. American Journal of Physiology-Legacy Content. 1952;169(1):229–35. https://doi.org/10.1152/ajplegacy.1952.169.1.229.
43. Paintal AS. A study of gastric stretch receptors; their role in the peripheral mechanism of satiation of hunger and thirst. J Physiol (Lond). 1954;126(2):255–70. https://doi.org/10.1113/jphysiol.1954.sp005207.
44. Mion F, Napoléon B, Roman S, et al. Effects of intragastric balloon on gastric emptying and plasma ghrelin levels in non-morbid obese patients. Obes Surg. 2005;15(4):510–6. https://doi.org/10.1381/0960892053723411.
45. Martinez-Brocca MA, Belda O, Parejo J, et al. Intragastric balloon-induced satiety is not mediated by modification in fasting or postprandial plasma ghrelin levels in morbid obesity. Obes Surg. 2007;17(5):649. https://doi.org/10.1007/s11695-007-9109-z.
46. Shiiya T, Nakazato M, Mizuta M, et al. Plasma ghrelin levels in lean and obese humans and the effect of glucose on ghrelin secretion. J Clin Endocrinol Metab. 2002;87(1):240–4. https://doi.org/10.1210/jcem.87.1.8129.
47. Sander B, Arantes VN, Alberti L, Neto MG, Grecco E, Souza TF. 550 Long-term effect of intragastric balloon in the management of obesity. Gastrointestinal Endoscopy. 2017;85(5, Supplement):AB83. https://doi.org/10.1016/j.gie.2017.03.113.
48. Ruban A, Stoenchev K, Ashrafian H, Teare J. Current treatments for obesity. Clin Med (Lond). 2019;19(3):205–12. https://doi.org/10.7861/clinmedicine.19-3-205.
49. Kumar RB, Aronne LJ. Review of multimodal therapies for obesity treatment: Including dietary, counseling strategies, and pharmacologic interventions. Techniques in Gastrointestinal Endoscopy. 2017;19(1):12–7. https://doi.org/10.1016/j.tgie.2016.11.003.
50. Gandarillas M, Hodgkinson SM, Riveros JL, Bas F. Effect of three different bariatric obesity surgery procedures on nutrient and energy digestibility using a swine experimental model. Exp Biol Med (Maywood). 2015;240(9):1158–64. https://doi.org/10.1177/1535370214567635.
51. Lupoli R, Lembo E, Saldalamacchia G, Avola CK, Angrisani L, Capaldo B. Bariatric surgery and long-term nutritional issues. World J Diabetes. 2017;8(11):464–74. https://doi.org/10.4239/wjd.v8.i11.464.
52. Moura D, Oliveira J, Moura EGHD, et al. Effectiveness of intragastric balloon for obesity: A systematic review and meta-analysis based on randomized control trials. Surgery for Obesity and Related Diseases. 2016;12(2):420–9. https://doi.org/10.1016/j.soard.2015.10.077.
53. Do TN, En T, Seah T, Yu HK, Phee SJ. Development and Testing of a Magnetically Actuated Capsule Endoscopy for Obesity Treatment. PLoS one. 2016;11(1):1–24. doi:https://doi.org/10.1371/journal.pone.0148035
54. Dumonceau J-M. Evidence-based review of the Bioenterics intragastric balloon for weight loss. Obes Surg. 2008;18(12):1611–7. https://doi.org/10.1007/s11695-008-9593-9.
55. New weight loss pill that expands in your stomach: is it safe? Healthline. Published 19 Apr 2019. https://www.healthline.com/health-news/plenty-weight-loss-pill. Accessed 13 Aug 2020.
56. Newly approved weight loss device blocks the vagus nerve. EndocrineWeb. https://www.endocrineweb.com/professional/obesity/newly-approved-weight-loss-device-blocks-vagus-nerve. Accessed 13 Aug 2020.
57. Bazerbachi F, Vargas Valls EJ, Abu Dayyeh BK. Recent Clinical Results of Endoscopic Bariatric Therapies as an Obesity Intervention. Clin Endosc. 2017;50(1):42–50. https://doi.org/10.5946/ce.2017.013.
58. Sharaiha R. Managing Obesity With Endoscopic Sleeve Gastroplasty. Gastroenterol Hepatol (N Y). 2017;13(9):547–9.
59. Norén E, Forssell H. Aspiration therapy for obesity; a safe and effective treatment. BMC Obes. 2016;3 https://doi.org/10.1186/s40608-016-0134-0.
60. Spring B, Schneider K, McFadden HG, et al. Multiple Behavior Change in Diet and Activity: A Randomized Controlled Trial Using Mobile Technology. Arch Intern Med. 2012;172(10):789–96. https://doi.org/10.1001/archinternmed.2012.1044.
61. Vibration: origins, effects, solutions | Galen Carol Audio | Galen Carol Audio. https://www.gcaudio.com/tips-tricks/vibration-origins-effects-solutions/. Accessed 13 Aug 2020.
62. Equen M, Roach G, Brown R, Bennett T. Magnetic Removal of Foreign Bodies from the Esophagus, Stomach, and Duodenum. AMA Arch Otolaryngol. 1957;66(6):698–706. https://doi.org/10.1001/archotol.1957.03830300078007.
63. The use of magnets in the control of traumatic gastritis of cattle. - Abstract – Europe PMC. https://europepmc.org/article/med/13366840. Accessed 13 Aug 2020.
64. Yim S, Sitti M. Shape-Programmable Soft Capsule Robots for Semi-Implantable Drug Delivery. IEEE Transactions on Robotics. 2012;28(5):1198–202. https://doi.org/10.1109/TRO.2012.2197309.
65. Lien G, Liu C, Jiang J, Chuang C, Teng M. Magnetic Control System Targeted for Capsule Endoscopic Operations in the Stomach—Design, Fabrication, and in vitro and ex vivo Evaluations. IEEE Transactions

on Biomedical Engineering. 2012;59(7):2068–79. https://doi.org/10.1109/TBME.2012.2198061.
66. Rahman I, Afzal NA, Patel P. The role of magnetic assisted capsule endoscopy (MACE) to aid visualisation in the upper GI tract. Computers in Biology and Medicine. 2015;65:359–63. https://doi.org/10.1016/j.compbiomed.2015.03.014.
67. Keller J, Fibbe C, Volke F, et al. Remote magnetic control of a wireless capsule endoscope in the esophagus is safe and feasible: results of a randomized, clinical trial in healthy volunteers. Gastrointestinal Endoscopy. 2010;72(5):941–6. https://doi.org/10.1016/j.gie.2010.06.053.
68. Gottlieb KT, Banerjee S, Barth BA, et al. Magnets in the GI tract. Gastrointestinal Endoscopy. 2013;78(4):561–7. https://doi.org/10.1016/j.gie.2013.07.020.
69. Rahman I, Kay M, Bryant T, et al. Optimizing the performance of magnetic-assisted capsule endoscopy of the upper GI tract using multiplanar CT modelling. Eur J Gastroenterol Hepatol. 2015;27(4):460–6. https://doi.org/10.1097/MEG.0000000000000312.
70. Gabriel S, Thompson WM, Bhar A, Swadene L, Ashley D. Development and Technology Transfer of the Syncro Blue Tube (Gabriel) Magnetically Guided Feeding Tube. Macon: Syncro Medical Innovations, Inc.; 2017. https://apps.dtic.mil/sti/citations/AD1038950. Accessed 14 Aug 2020.
71. Gabriel SA, McDaniel B, Ashley DW, Dalton ML, Gamblin TC. Magnetically guided nasoenteral feeding tubes: a new technique. Am Surg. 2001;67(6):544–8; discussion 548–549.
72. Gabriel SA, Ackermann RJ. Placement of nasoenteral feeding tubes using external magnetic guidance. Journal of Parenteral and Enteral Nutrition. 2004;28(2):119–22. https://doi.org/10.1177/0148607104028002119.
73. Rivas H, Robles I, Riquelme F, et al. Magnetic Surgery. Ann Surg. 2018;267(1):88–93. https://doi.org/10.1097/SLA.0000000000002045.
74. Pressure. http://hyperphysics.phy-astr.gsu.edu/hbase/press.html#pre. Accessed 8 Mar 2020.
75. Nakayama S, Hasegawa S, Nagayama S, et al. The importance of precompression time for secure stapling with a linear stapler. Surg Endosc. 2011;25(7):2382–6. https://doi.org/10.1007/s00464-010-1527-7.
76. Cartmill JA, Shakeshaft AJ, Walsh WR, Martin CJ. High Pressures Are Generated at the Tip of Laparoscopic Graspers. Australian and New Zealand Journal of Surgery. 1999;69(2):127–30. https://doi.org/10.1046/j.1440-1622.1999.01496.x.
77. Shakeshaft AJ, Cartmill JA, Walsh WR, Martin CJ. A curved edge moderates high pressure generated by a laparoscopic grasper. Surg Endosc. 2001;15(10):1232–4. https://doi.org/10.1007/s00464-001-0036-0.
78. Rapaccini GL, Aliotta A, Pompili M, et al. Gastric wall thickness in normal and neoplastic subjects: a prospective study performed by abdominal ultrasound. Gastrointest Radiol. 1988;13(1):197–9. https://doi.org/10.1007/BF01889058.